Journal of Soils and Sediments (2024) 24:1814–1825
https://doi.org/10.1007/s11368-023-03591-y

SEDIMENT ENVIRONMENT AND POLLUTION CONTROL 2022

Phosphorus release flux and mechanism at the sediment–water interface of the Three Gorges Reservoir in the Yangtze River basin, China

Jiaojiao Yang[1,2] · Yiming Ma[1] · Shanze Li[3] · Jingfu Wang[1,2] · Zuxue Jin[1,2] · Danhao Li[1,4] · Yuchun Wang[1,3]

Received: 12 March 2023 / Accepted: 24 June 2023 / Published online: 5 July 2023

Abstract

Purpose The Three Gorges Reservoir (TGR) is the largest water conservation project in the world but suffers from harmful algal blooms (HABs) currently. A large amount of phosphorus (P) has accumulated in the sediment due to the construction of the Three Gorges Dam. Phosphorus release from sediment may provide an important P source for overlying water that further triggers HABs. This study aimed to evaluate the contribution of sediment internal P and reveal the mechanisms controlling sediment P release.

Material and methods Chemical sequential extraction approach and diffusive gradients in thin films (DGT) techniques were employed to determine the P fractions in sediments and the vertical distribution of P, iron (Fe), and sulfur (S) at the sediment–water interface (SWI).

Results and discussion Results indicated that the total P content in the sediments of the TGR is high, with a mean content of 1368 mg kg^{-1}. The P concentration of different fractions in sediments followed the order HCl-P > NaOH-P > BD-P. The averaged P release flux at the SWI was estimated at 0.42 mg m^{-2} day^{-1}, suggesting that sediment P release is a potential P source for the overlying water. Significant positive relationships between DGT-P and DGT-Fe concentrations from sampling sites Wushan County (WS), Zigui County (ZG), and Xiangxi River (XX) were observed with correlation coefficients (R^2) of 0.91, 0.39, and 0.29, respectively. Furthermore, DGT-P and DGT-S concentrations were also significantly positively correlated at the sampling sites WS, ZG, and XX, with R^2 of 0.71, 0.87, and 0.50, respectively.

Conclusion The internal P load is severe in the TGR. The reductive dissolution of Fe–P is likely one of the main mechanisms causing P release in the sediments. Furthermore, sulfate reduction associated coprecipitation with Fe promotes the release of Fe–P. These results provide important scientific and technical support for the mitigation of internal P pollution in large deep-water reservoirs.

Keywords Phosphorus · Sediment–water interface · Chemical sequential extraction · Diffusive gradients in thin films (DGT) · Three Gorges Reservoir

1 Introduction

Anthropogenic activities such as urbanization, industrialization, and climatic changes have significantly aggravated water eutrophication in approximately 63% of lakes and reservoirs worldwide (Wang et al. 2018a). Internal phosphorus (P) is recognized as one of the key limiting factors for water eutrophication in aquatic ecosystems when external P inputs are effectively controlled (Lewis et al. 2011; Schindler et al. 2016; Chen et al. 2018). Therefore, internal P release has attracted increasing attention recently. Most of P released from the sediment is soluble inorganic P, which is a critical P source for algae growth and proliferation in lakes and reservoirs (Correll 1998). P

Responsible editor: Lu Zhang

✉ Jingfu Wang
wangjingfu@vip.skleg.cn

[1] State Key Laboratory of Environmental Geochemistry, Institute of Geochemistry, Chinese Academy of Sciences, Guiyang 550081, China

[2] University of Chinese Academy of Sciences, Beijing 100049, China

[3] Institute of Water Resources and Hydropower Research, State Key Laboratory of Basin Water Cycle Simulation and Regulation, Beijing 100038, China

[4] State Key Laboratory of Eco-Hydraulics in Northwest Arid Region of China, Xi'an University of Technology, Xi'an 710048, China

release from sediment is estimated to sustain eutrophication in surface water for over a decade (Paytan et al. 2017). Consequently, understanding the flux and mechanisms of internal P release is imperative to mitigate eutrophication and enhance water quality in lakes and reservoirs.

Over the past decades, P release processes and mechanisms have been the subject of extensive investigation, especially at the sediment−water interface (SWI). It has been reported that P release from sediment is controlled by temperature (T), dissolved oxygen (DO), pH, hydrodynamic conditions, microbial activity, and redox potential (Andrieux et al. 2008; Jiang et al. 2008). High temperature can promote the releasing rate of P from sediment (Jiang et al. 2008). Under aerobic conditions, dissolved P from pore water and overlying water could be adsorbed by iron (hydro) oxides, thereby considerably limiting the releasing rate of P from the sediment (Jiang et al. 2008; Chen et al. 2019). In contrast, anaerobic or anoxic conditions favor the release of P from sediment (enhanced P-releasing rate), thereby stimulating algal blooms in aquatic ecosystems. Biological activities can modify the microenvironment surrounding the sediment, thereby promoting sediment P release (Jiang et al. 2008).

Phosphorus release from sediment is conventionally believed to occur within a millimeter to centimeter range at the SWI, but traditional centimeter-scale sampling methods cannot accurately monitor sediment P release (Ding et al. 2012). In recent years, the rapid development of in situ passive sampling techniques has provided a powerful strategy for analyzing the temporal and spatial distributions of P concentration at the SWI (Ding et al. 2016; Wang et al. 2018b; Chen et al. 2019). Studies have demonstrated that P transport in sediments is closely associated with the geochemical cycling of iron (Fe) and sulfur (S) (Zhou et al. 2023). For example, Ding et al. (2016) investigated 16 sites in Taihu Lake, China, utilizing diffusive gradients in thin films (DGT), and revealed that reductive dissolution of Fe–P was the principal mechanism for sediment P release. Similarly, Chen et al. (2019) established a significantly positive correlation between reactive P and reactive Fe in sediments at Hongfeng Reservoir in southwest China. However, Yu et al. (2022) showed that the reductive dissolution of Fe–P from sediment did not significantly contribute to the internal P loading in grassland-type lakes. Generally, the SWI environment in deep-water lakes is anoxic, which can provide positive feedback featuring bottom water hypoxia, enhanced internal P release, and increased primary productivity of the lake. It is important to note that most of the above studies were conducted in shallow lakes. Little is known about the release flux and mechanism of P at the SWI in deep reservoirs, especially those constructed by large hydraulic projects.

China has constructed approximately 100,000 reservoirs, of which 9215 are large- and medium-sized reservoirs, accounting for about one-fourth of the available global reservoirs (Mulligan et al. 2020; Zhu et al. 2020). The Three Gorges Reservoir (TGR) that originates from the Yangtze River basin is the world's largest hydroelectric gravity dam with a total reservoir length of 625 km. The dam intercepts large amounts of nutrients from the upstream rivers, which accumulate in the reservoir and thereby result in frequent water eutrophication (Mueller and Mitrovic 2015; Lei et al. 2021). Approximately 12% of riverine P loads were intercepted in reservoir sediment by the year 2000 globally, and this percentage is projected to rise to 17% by 2030, primarily in the basins of the Yangtze, Mekong, and Amazon rivers (Maavara et al. 2015). However, the fractions, release flux, and mechanisms of P at the SWI in reservoirs have not been systematically studied, thereby constraining the scientific evaluation of internal P pollution.

In this study, the chemical sequential extraction was used to analyze sediment P fractions in the TGR. A DGT technique was used to obtain the spatial distributions of P, Fe, and S concentrations, which can be used to calculate internal P release flux at the SWI. The main objectives of this study were to (1) elucidate the spatial distribution of P fractions in sediments; (2) quantify the P release flux at the SWI; and (3) establish the microscopic mechanisms of sediment P release. These results will provide profound insights and theoretical basis for risk assessment and management of internal P pollution in the TGR.

2 Materials and methods

2.1 Study site

The TGR area spans from Jiangjin District in Chongqing to Yichang City in Hubei province and covers 20 county-level administrative units. The reservoir has a surface area of about 1080 km^2, an average depth of about 70 m, and a maximum depth near the dam of about 170 m (Wu et al. 2003). The reservoir water storage capacity is estimated at 39.3 billion m^3, of which 22.15 billion m^3 is for flood control (Bao et al. 2015; Gao et al. 2023). Despite the Three Gorges Dam has great economic value, it confronts environmental challenges. For instance, Xiangxi River, a major tributary of the TGR, has encountered significant environmental problems like widespread harmful algal blooms (Wang et al. 2015; Luo et al. 2022). Among the 20 counties, Wushan County is located in the mainstream through which the TGR must pass. Since constant sedimentation is expected to have a profound effect on the landscape, it is important to understand

the current status of P pollution in the TGR. To assess the P pollution status within the TGR, Wushan County (WS), Xiangxi River (XX), and Zigui County (ZG) were identified as sampling sites, due to their important geographical roles.

2.2 Sample collection

Core sampling was performed in September 2022. Three sediment cores were collected from WS, ZG, and XX in the TGR, utilizing a gravity sampler with an internal diameter of 11 cm (Fig. 1). The water interface was kept clear during the collection of the sediment cores to reduce experimental inaccuracies and facilitate observation. Once sample cores were collected, the bottom was sealed with a rubber stopper, and a DGT probe was inserted vertically into the surface sediment from the top; the water temperature was recorded. After 24 h, the DGT probe was extracted from the sediment core, immediately rinsed with ultrapure water, sealed, enshrouded in aluminum foil, and subsequently refrigerated until returning back to the laboratory for chemical analysis. After the removal of the DGT probe, the sediment core was cut to 1 cm and placed in the centrifuge tube. The surface water (0.5 m from the water surface), mid-water (water depth at 20–30 m), and bottom water (1 m from sediment) were collected using a Niskin water sampler. A multi-parameter water-quality monitor (YSI6600V2, YSI Inc., Yellow Springs, USA) was used to monitor the water temperature (T), dissolved oxygen (DO), and pH of the water body.

2.3 Preparation and field deployment of the DGT probe

In this study, we used the ZrO-CA DGT (Easy Sensor Ltd., Nanjing, China) to simultaneously acquire a two-dimensional high-resolution data for dissolved S (DGT-S), and a one-dimensional high-resolution data for dissolved active P (DGT-P) and dissolved Fe (DGT-Fe) at the SWI. As described above, after collecting the sediment core, the DGT probe was inserted vertically into the surface sediment from the top, leaving a 5 cm space between the top of the probe window and the SWI. After 24 h, the DGT probe was removed, sealed, refrigerated, and transported to the lab for chemical analysis. Three parallel column cores were collected from each site, and visual inspection revealed no significant differences between the parallel cores (including sediment color, density, and grain layer), so one of the cores was selected for the DGT study.

2.4 Chemical analysis

2.4.1 Water chemistry and sediment properties

The molybdenum blue colorimetry method was used to determine the total P (TP) and total dissolved P (TDP) concentrations in water samples (Murphy and Riley 1962). Total nitrogen (TN) and total dissolved nitrogen (TDN) concentrations were determined by alkaline potassium persulfate digestion and ultraviolet spectrophotometry (HJ636-2012).

The surface sediments (0–5 cm) were digested with mixed acid (HNO_3-HF) to determine Fe, Mn, Ca, and Al

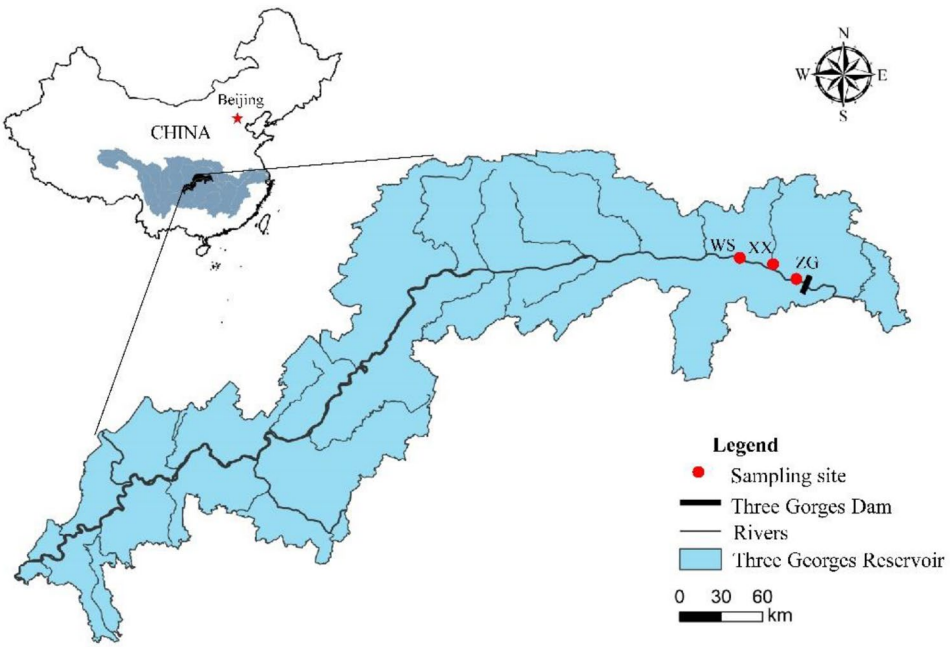

Fig. 1 The study area and sampling sites in the Three Gorges Reservoir (TGR) of the Yangtze River in China

contents (Zhang et al. 2020). The pretreatment procedures included weighing 0.5 g of the sediment sample into a Teflon digestion tube followed by the addition of 0.8 mL HF and 1 mL HNO_3. The Teflon digestion tube was then placed in a steel tank and heated in an oven (at 180–190℃) for 24–30 h. After cooling, the Teflon digestion tube was placed on an electric hot plate and allowed to evaporate the contents until dry (at 140 °C). Thereafter, a small amount of HNO_3 (< 1 mL) was added, followed by adding 2 mL of HNO_3 and 3 mL of ultrapure water, which was then heated in a sealed oven with a lid (at 140 °C) for 4–5 h. It was later cooled to a achieve constant volume of 100 mL. The samples were analyzed using inductively coupled plasma–optical emission spectrometry (ICP-OES; Vista MPX, Varian, USA).

Following freeze-drying, grinding, and sieving (through 100-mesh) of the surface sediments (0–5 cm), the P fractions were analyzed according to the sequential chemical extraction method developed by Hupfer et al. (1995) with five extraction steps. First, (1) NH_4Cl-P extraction, 25 mL of 1 M NH_4Cl was added to 0.2 g sediment sample and shaken for 0.5 h; (2) BD-P extraction, the residue extract was mixed with 25 mL of 0.11 M $NaHCO_3$ and 0.11 M of $Na_2S_2O_4$ solution and shaken for 1 h; (3) NaOH-P extraction, 25 mL of 1 M NaOH was added to the residue extract and shaken for 16 h; (4) HCl-P extraction, 25 mL of 0.5 M HCl was added to the residue extract shaken for 16 h; and (5) after freeze-drying, the residue extract was ashed at 500 ℃ for 2 h and transferred to a 50 mL centrifuge tube, where it was further cooled to the room temperature. The Residual-P was extracted by adding 25 mL of 1 M HCl and shaken for 16 h. The concentrations of P in all extracts described above were determined by the molybdenum blue colorimetric method (Murphy and Riley 1962). To minimize operational and other potential errors, three replicate experiments were conducted to take the average of physio-chemical property for sediment samples and water samples.

2.4.2 Analysis of the DGT

The fixed film was removed from the DGT device using plastic tweezers and their surfaces were dried using a filter paper and placed on the scanner with the sedimentation side facing downwards. The scanned image (resolution at 300 dpi) was converted to grayscale using ImageJ software. The grayscale was further converted into the cumulative amount per unit (M) area of S by the correction curve. Therefore, the information on the submillimeter distribution of S at SWI was obtained. The calibration curve was shown in Eq. 1, as described by Ding et al. (2012):

$$y = -167.3e^{-x/6.51} + 214.6 \quad (1)$$

where x is the cumulative amount per unit area of the fixed film (M) in g cm^{-2}.

The scanned fixed membranes were sectioned at 2 mm intervals using a ceramic knife. The sections were then transferred into a 1.5 mL centrifuge tube. The Fe was extracted using 0.8 mL of 1 mol L^{-1} nitric acid for 16 h. The concentration of Fe in the extract was determined using an Epoch microplate spectrophotometer (Bio Tek, Winooski, VT). Thereafter, the residual DGT membrane was extracted using 0.8 mL of a 1 mol/L sodium hydroxide solution for 16 h. The concentration of P in the extract was determined by the molybdenum blue colorimetric method (Murphy and Riley 1962; Wang et al. 2017). Three replicates were performed for each sample to reduce the experimental errors. The accumulation (M) of Fe and P in fixed films was calculated using Eq. 2 (Wang et al. 2016a).

$$M = \frac{C_e V_e}{f_e} \quad (2)$$

where C_e is the concentration of the extracted solution, V_e is the volume of the extracted agent, and f_e is the extraction rate.

The concentrations of DGT-S, DGT-Fe, and DGT-P in the sediment were calculated by Eq. 3 (Wang et al. 2016a):

$$C_{\mathrm{DGT}} = \frac{M\Delta g}{D\mathrm{A}t} \quad (3)$$

where C_{DGT} represents the concentration (mg L^{-1}) of the target substance; M signifies the cumulative amount (μg cm^{-2}) of the ZrO-CA DGT film over the sampling time; Δg is the thickness of the thin film diffusion layer (cm); D is the diffusion coefficient at the corresponding temperature (cm^2 s^{-1}); A is the sampling area (cm^2); and T is the sampling time (s).

2.5 Data analysis

Fick's first law and the DGT-P concentration distribution near SWI were used to estimate the apparent diffusion flux from P at the SWI (Ding et al. 2015).

$$F_{\mathrm{d}}=\mathrm{J}_W + \mathrm{J}_S = -D_{\mathrm{W}}\left(\frac{\delta \mathrm{C}_{\mathrm{DGT}}}{\delta \mathrm{X}_{\mathrm{w}}}\right)_{x=0} - \varphi D_{\mathrm{S}}\left(\frac{\delta \mathrm{C}_{\mathrm{DGT}}}{\delta \mathrm{X}_{\mathrm{s}}}\right)_{\mathrm{x=0}} \quad (4)$$

where F_{d} is the diffusive flux at the SWI (mg m^{-2} day^{-1}); φ is the porosity of surface sediments; D_{W} and D_{S} are the diffusion coefficients of phosphate in overlying water and sediment, respectively; $\left(\frac{\delta C_{DGT}}{\delta X_w}\right)_{x=0}$ and $\left(\frac{\delta C_{DGT}}{\delta X_s}\right)_{x=0}$ are the concentration gradients of DGT-P in overlying water and sediment, respectively.

To obtain an accurate estimation of P release flux, the concentration gradients were calculated from the profiles

with tiny fluctuations in the DGT-P concentration. The diffusion coefficient for phosphate in sediments was calculated according to Eq. 5 below (Ullman and Aller 1982):

$$D_S = \frac{D_W}{\varphi F} \quad (5)$$

where φ is the porosity of surface sediments; F is the formation resistivity coefficient; D_W is the diffusion coefficient of phosphate in water, as determined by temperature; the formation resistivity coefficient was determined by the porosity of the sediment (φ), $F = 1/\varphi^3$, when $\varphi \geq 0.7$; and $F = 1/\varphi^2$, when $\varphi < 0.7$ (Yuan-Hui and Gregory 1974; Ullman and Aller 1982).

3 Results and discussion

3.1 Water chemistry

The water body profile exhibits a temperature of around 28 °C, and the water temperature slowly decreases from the surface to the bottom. Due to the strong hydrodynamic effect in the WS, the thermal stratification of the water body is not obvious (Fig. 2a). The average pH of bottom water is 7.67 (Fig. 2b), which could be related to the enhanced degradation of organic species. The DO concentrations are observed to be above 5 mg L^{-1} under aerobic conditions (Fig. 2c).

Nitrogen and P are mainly presented in dissolved forms. TDN and TDP account for 96.9% and 94.2% of their corresponding TN and TP, respectively (Fig. 3). The concentration of TP in the water body varies from 0.037 to 0.055 mg L^{-1} with an average of 0.044 mg L^{-1}, while the corresponding value of TN ranges from 1.29 to 1.50 mg L^{-1} with 1.38 mg L^{-1} as the average level. Besides, it is observed that the concentration of N and P in the bottom water is greater than that in the surface water, which could be contributed to the sediment N and P release.

3.2 Sediment properties and phosphorus fractions

The highest content of Al is found at the depth of 0–5 cm of the sediments, which ranges from 7.24 to 9.67% with an average level of 8.35%. With respect to Fe, Ca, and Mn, the corresponding values range 4.71–6.87% (averagely 5.33%), 2.94–5.14% (averagely 3.90%), and 0.09–0.14% (averagely 0.11%), respectively (Table 1). Accordingly, a comparison of the contents of Al, Fe, Ca, and Mn in the sediments shows a descending order as WS > ZG > XX.

The variations in P fractions in surface sediments are shown in Fig. 4. The TP contents in sediment of the TGR vary from 1284 to 1476 mg kg^{-1} (mean value of 1368 mg kg^{-1}), which are much lower than that in moderate eutrophication lake sediment such as Lake Dianchi (2050 mg kg^{-1}), but significantly higher than that in Lake Erhai sediment (999 mg kg^{-1}) and Taihu Lake (540 mg kg^{-1}) (Zhang et al. 2013; Chen et al. 2020). Contents of TP in sediments in TGR indicate that the sediment in the TGR is characterized by high amounts of internal P load. There is no significant difference in the P content of surface sediment in the TGR area (Fig. 4). Following a descending order of the P content in sediment, the different P forms are in the order of HCl-P > NaOH-P > Rest-P > BD-P > NH_4Cl-P, which is consistent with the findings from previous work (Wang et al. 2015).

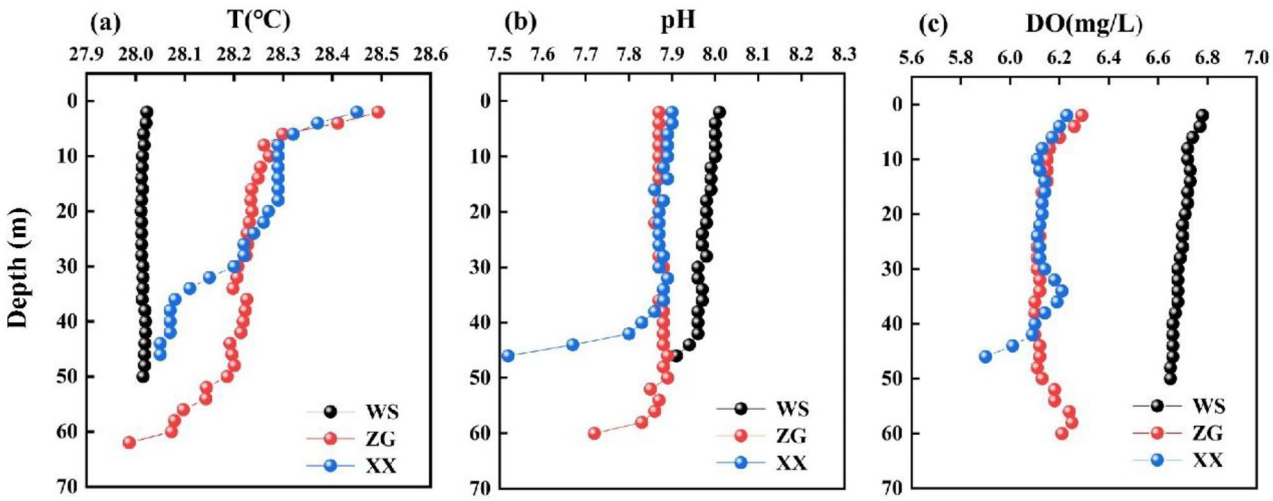

Fig. 2 Vertical profiles of temperature (**a**), pH (**b**), and dissolved oxygen content (**c**) at the sampling sites of the Three Gorges Reservoir (TGR) in China

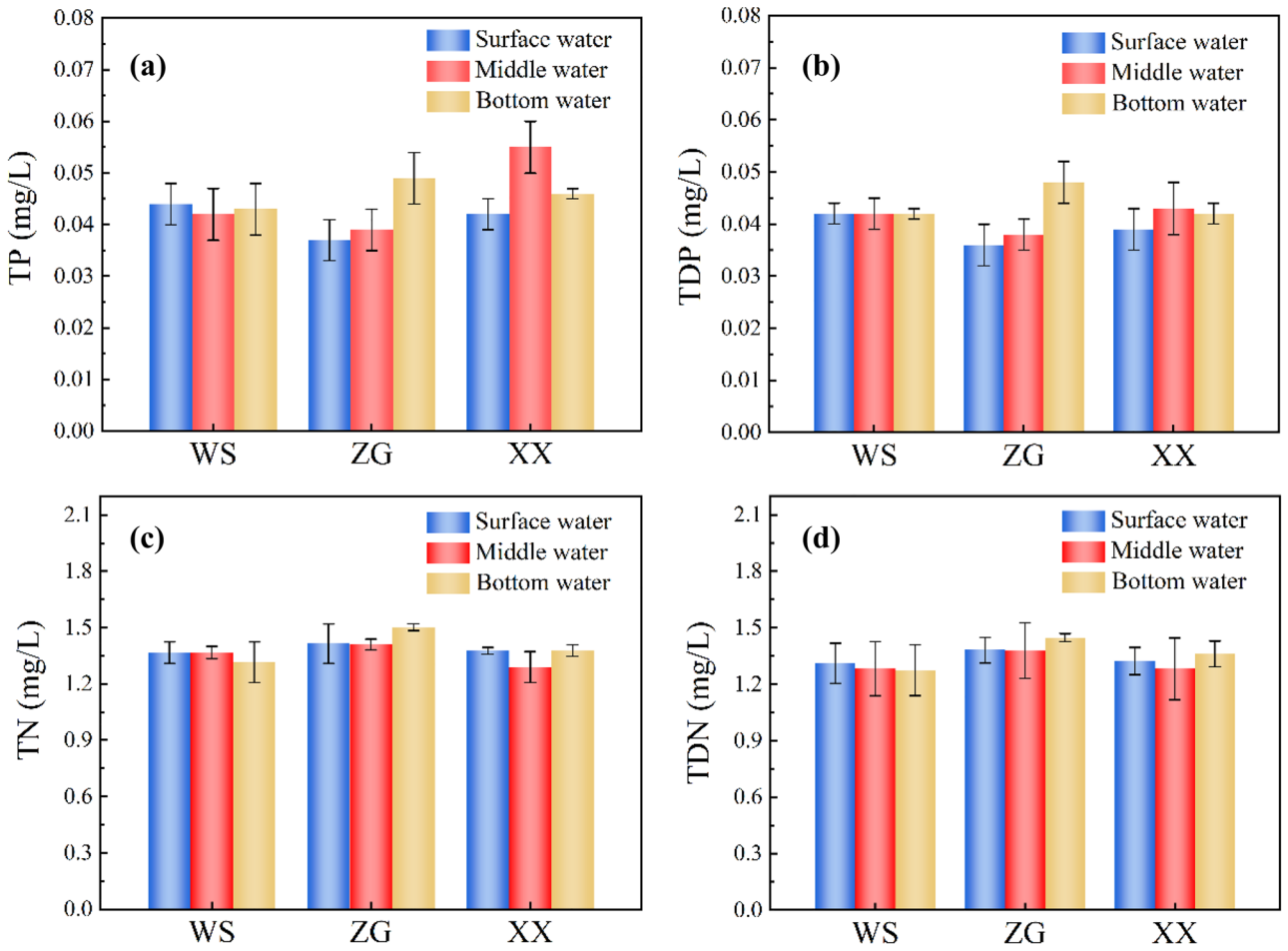

Fig. 3 Total phosphorus (TP; **a**), total dissolved phosphorus (TDP; **b**), total nitrogen (TN; **c**), and total dissolved nitrogen (TDN; **d**) concentrations in surface, middle, and bottom water at the sampling sites (WS, ZG, and XX) of the Three Gorges Reservoir (TGR) in China. The error bars represented the standard deviations of triplicate experiments

The contents of sediment HCl-P range from 503 to 766 mg kg^{-1}, accounting for 39.4 to 49.0% of TP (Fig. 4). The HCl-P is mainly fixed in calcium and magnesium minerals that have strong stability; therefore, the HCl-P pool serves as the permanent burials of P in sediments (Hupfer et al. 1995). However, HCl-P can be released to some extent under acidic conditions (Wang et al. 2021), whereas the water body in the TGR is slightly alkaline (pH > 7.5), and thus it is difficult for HCl-P to participate in the P cycle. The high content of sediment HCl-P in the TGR can be attributed to the recharge of calcareous terrain on both sides of the river and the coprecipitation of a large amount of calcium ions (Sun et al. 2009; Mu et al. 2020).

The NaOH-P is considered to be associated with Fe and Al (hydro)oxides so that there are relatively less stable than HCl-P (Christophoridis and Fytianos 2006). The content of NaOH-P ranges from 275 to 690 mg kg^{-1}, accounting for 25.6–36.5% of TP (Fig. 4). The Res-P is mainly composed of refractory organic P and inert inorganic P (Rydin 2000). The content of Res-P varies from 172 to 169 mg kg^{-1} and accounts for 12.0–19.6% of TP. Besides, BD-P is mainly found on the surfaces of Fe (III) and Mn (hydro) oxides (Christophoridis and Fytianos 2006); its content in the sediment varies between 112 and 151 mg kg^{-1}. The NH_4Cl-P represents the loosely adsorbed P in the sediment and its contents range from 6.38 to 13.40 mg kg^{-1}. Sediment NH_4Cl-P has the lowest average content value among the five different P species/forms, indicating an insignificant contribution of sediment NH_4Cl-P to sediment TP (Fig. 4).

Bioavailable P (BAP) is composed of $NHCl_4$-P, BD-P, and NaOH-P in sediment, which could be absorbed and utilized by organisms. Therefore, BAP is regarded as a potential P source for overlying water (Tu et al. 2019). The content of BAP in the surface sediments ranges from 480 to 629 mg kg^{-1}, accounting for 36.2–45.9% of the TP in the sediments. Since BAP is highly bioavailable, the content of sediment BAP is relatively low in flora- and

Table 1 Contents of Al, Fe, Ca, and Mn in the surficial sediments of the sampling sites in the Three Gorges Reservoir (TGR)

Sample	Depth (cm)	Al (%)	Fe (%)	Ca (%)	Mn (%)
WS	0–1	9.04	5.22	4.06	0.12
	1–2	8.89	5.16	4.05	0.12
	2–3	8.02	5.34	3.97	0.12
	3–4	8.71	5.32	3.85	0.12
	4–5	9.02	5.20	3.79	0.11
ZG	0–1	9.67	6.18	5.26	0.14
	1–2	8.37	4.71	5.14	0.09
	2–3	8.86	5.02	3.91	0.10
	3–4	7.50	5.64	3.77	0.11
	4–5	9.44	6.87	4.52	0.13
XX	0–1	7.75	5.02	3.58	0.11
	1–2	7.74	4.97	3.36	0.10
	2–3	7.24	5.20	3.04	0.09
	3–4	7.31	5.09	2.94	0.09
	4–5	7.72	5.05	3.25	0.09
Standard	-	5.94	2.87	0.01	0.05

fauna-dominated reservoir, and high in eutrophic water body polluted by human activities (Yu et al. 2022). On the other hand, the contents of $NHCl_4$-P, BD-P, and NaOH-P in the sediments at XX (average value of 629 mg kg^{-1}) are obviously higher than those at WS (average value of 520 mg kg^{-1}) and ZG (average value of 480 mg kg^{-1}) (Fig. 4). This might be due to the shift of active P in the sediments caused by the transportation of fine-grained sediments towards the dam (Wu et al. 2016). In addition, the Xiangxi River is an influential tributary of the TGR. Agricultural non-point source pollution and domestic sewage discharges are likely to contribute to the accumulation of nutrients (Wang et al. 2015).

Table 2 The apparent diffusion fluxes of phosphorus at the sediment−water interface (SWI) in the Three Gorges Reservoir (TGR)

Sampling sites	WS	ZG	XX
Diffusion fluxes of P (mg m^{-2} day^{-1})	0.11	0.41	0.75

3.3 The influx of internal P loading at three sampling sites

Fick's first law and the DGT-P concentration distribution near SWI were used to estimate the apparent diffusion flux of P at the SWI. Sediment as a P source when P release flux is positive, indicating that P is released from the sediment to the overlying water (Ullman and Sandstrom 1987). Conversely, the sediment is a P sink, demonstrating that P enters the sediment from the water column (Moore et al. 1998). The P release flux at the SWI of the three sampling locations is listed in Table 2. The value of P release flux ranges

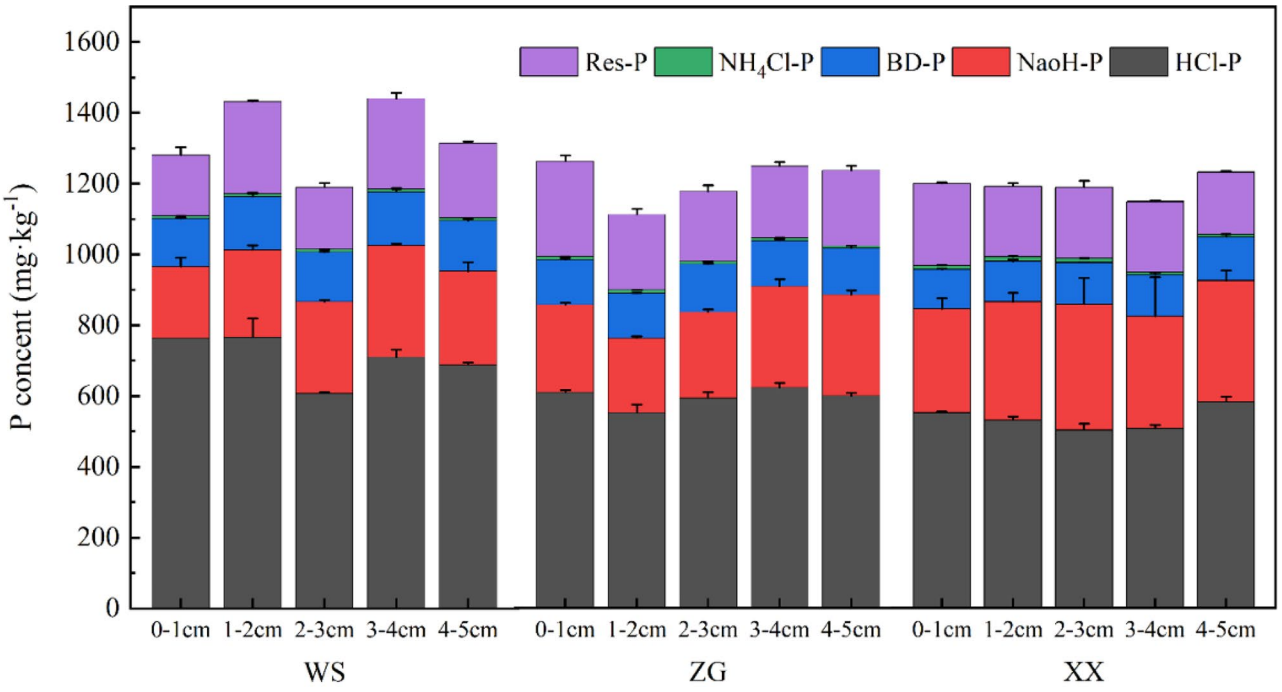

Fig. 4 Phosphorus concentration of different fractions in the surface sediments at the WS, ZG, and XX sampling sites in the Three Gorges Reservoir (TGR) in China. The error bars represented the standard deviations of triplicate experiments

from 0.11 to 0.75 mg m^{-2} day^{-1} with an average value of 0.42 mg m^{-2} day^{-1}. The P release flux from sediment in the TGR is higher than that in Wujiang River reservoirs, another tributary of the Yangtze River (such as Hongfeng Lake Reservoir, average value of 0.22 mg m^{-2} day^{-1}) and large shallow eutrophic lakes in eastern China (e.g., Taihu Lake, average level of 0.15 mg m^{-2} day^{-1}) (Ding et al. 2015; Chen et al. 2019). According to molecular diffusion theory (see M S1), the annual internal P flux in the Three Gorges Reservoir is estimated at 166 tons, and the contribution of annual internal P release to TP in the overlying water column reached 10%. These results suggest that the sediment is an essential P source for overlying water in the TGR.

There are many reasons responsible for the serious P pollution in the TGR. First, TGR is a river-like reservoir where large amounts of sediments have accumulated here, which were derived from the water and soil losses at both sides of the river. Therefore, an unstable and cool SWI was created (Li et al. 2021). Second, gravity flow is the main form of water exchange between the mainstream and the tributaries of the TGR, and the reverse action of the mainstream on the tributaries may promote the P release from the tributaries (Wang et al. 2015). This could explain why the P release flux of the tributary (XX) is higher than that of the mainstreams (WS and ZG). Moreover, the TGR locates in a population-intensive area. There is a large influx of anthropogenic P sources (including agricultural and industrial pollutions, as well as domestic sewage) (Liu et al. 2006). It could be concluded that the TGR has a large P load, high P release rate, and great pollution risk, highlighting the important urgency to control the P pollutions. Sediment P contaminations have been overlooked historically. Consequently, sediment P release in the TGR has become a serious problem in recent years. The continuous accumulation of P in sediments may significantly impact the water quality adversely, which is an issue deserving special attention from the government and the whole society.

3.4 Mechanism of phosphorus release at the sediment–water interface in the TGR

We selected three representative sampling points to compare the two-dimensional longitudinal distribution patterns of DGT-P, DGT-Fe, and DGT-S at the SWI in the mainstream (WS), dam (ZG), and tributary (XX) (Fig. 5). The concentrations of DGT-P, DGT-Fe, and DGT-S increase rapidly at the SWI, with a similar longitudinal trend. The concentration of DGT-P at the XX site, with a mean value of 0.18 mg L^{-1}, is significantly higher than that at the other two sampling sites. With the increase in the sediment depth, the concentration of DGT-P at the XX site first increases gradually to reach a peak value at the depth of 10 mm, and then decreases gradually to achieve a stable state (Fig. 5a-c). The concentration of DGT-Fe at the three sites reaches its peak value at the depth of 20 mm (Fig. 5d-f). The content variation of DGT-Fe in the sediments of ZG is extremely steep, with an average level of 3.02 mg L^{-1} and a maximum value of 9.49 mg L^{-1} at 2 cm depth. The mean concentration of DGT-S at the XX site (0.049 mg L^{-1}) is significantly higher than that at the WS (0.029 mg L^{-1}) and ZG sites (0.036 mg L^{-1}) (Fig. 5g-i).

The concentrations of DGT-P and DGT-Fe at WS, ZG, and XX sampling sites could be positively correlated, and the correlation coefficients (R^2) are 0.91, 0.39, and 0.29, respectively ($p < 0.05$; Fig. 6a-c). The correlation analysis shows that P and Fe are released simultaneously from sediment. Under aerobic conditions, Fe is present in the surface sediments mainly as Fe (III) hydroxide oxides, which can retain phosphate in FeOOH-P complexes (De et al. 2012), where the sediment acts as a P sink to immobilize phosphorus species from the overlying water. Due to the limited penetration depth of DO, the SWI of deep-water reservoirs often creates an anoxic environment, which enables the reductive dissolution of Fe in the sediment surface and therefore induces the release of Fe–P. The positive correlation between DGT-P and DGT-Fe has been observed in different reservoirs in the upper reaches of the Yangtze River (Ahlgren et al. 2005; Ding et al. 2016; Wang et al. 2018b; Chen et al. 2019). Our study shows that tributaries have the highest P release flux and the weakest correlation between DGT-P and DGT-Fe compared to mainstem and dams. It suggests that P release mechanisms may not be dominated by Fe, and that sediment re-suspension by hydrodynamic disturbances and organic P mineralization may be responsible in tributaries (Wu et al. 2019; Yu et al. 2022). Further investigation is needed to fully understand the unusual variations of the DGT-P and DGT-Fe in tributaries.

In addition, similar variations in sediment DGT-P and DGT-S concentrations are observed (Fig. 5g-i). In the profile, the concentrations of DGT-P and DGT-S are significantly positively correlated, and the correlation coefficients (R^2) are 0.71, 0.87, and 0.50, respectively ($p < 0.05$; Fig. 6g-i). It was reported previously that the geochemical cycling of P and Fe in sediments could be related to the reduction reaction caused by sulfate-reducing bacteria (SRB) (Roden and Zachara 1996). Under anoxic conditions, the reduction of Fe (II) species with SRB produces FeS precipitation, which reacts subsequently with sulfide to produce pyrite (FeS_2). This FeS_2 product can promote the reductive dissolution of Fe(III), which in turn induces

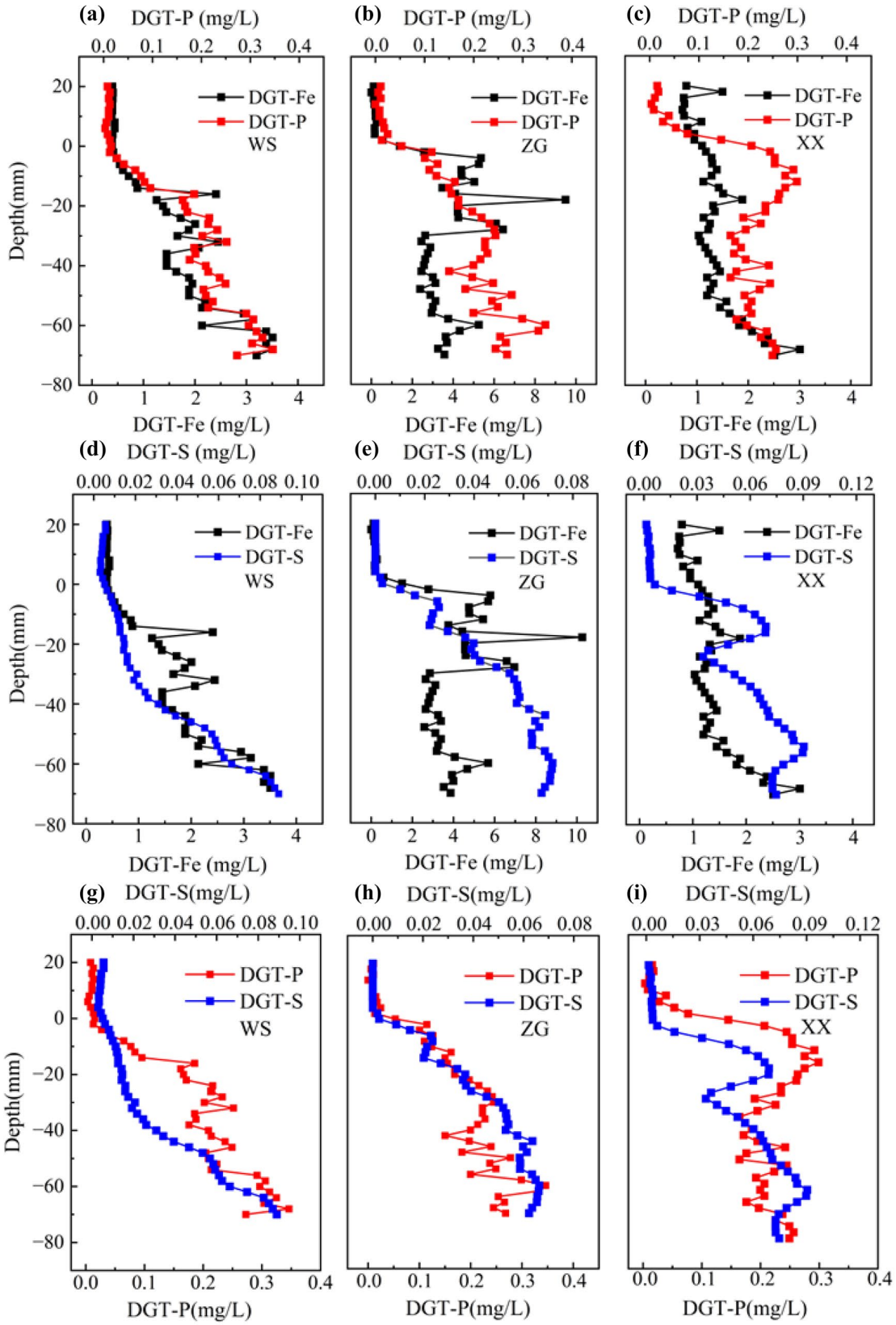

Fig. 5 Vertical concentration variations between DGT-P and DGT-Fe (**a**–**c**), DGT-S and DGT-Fe (**d**–**f**), and DGT-S and DGT-P (**g**–i) at the sediment–water interface (SWI) of the sampling sites (WS, ZG, and XX) in the Three Georges Reservoir (TGR) in China

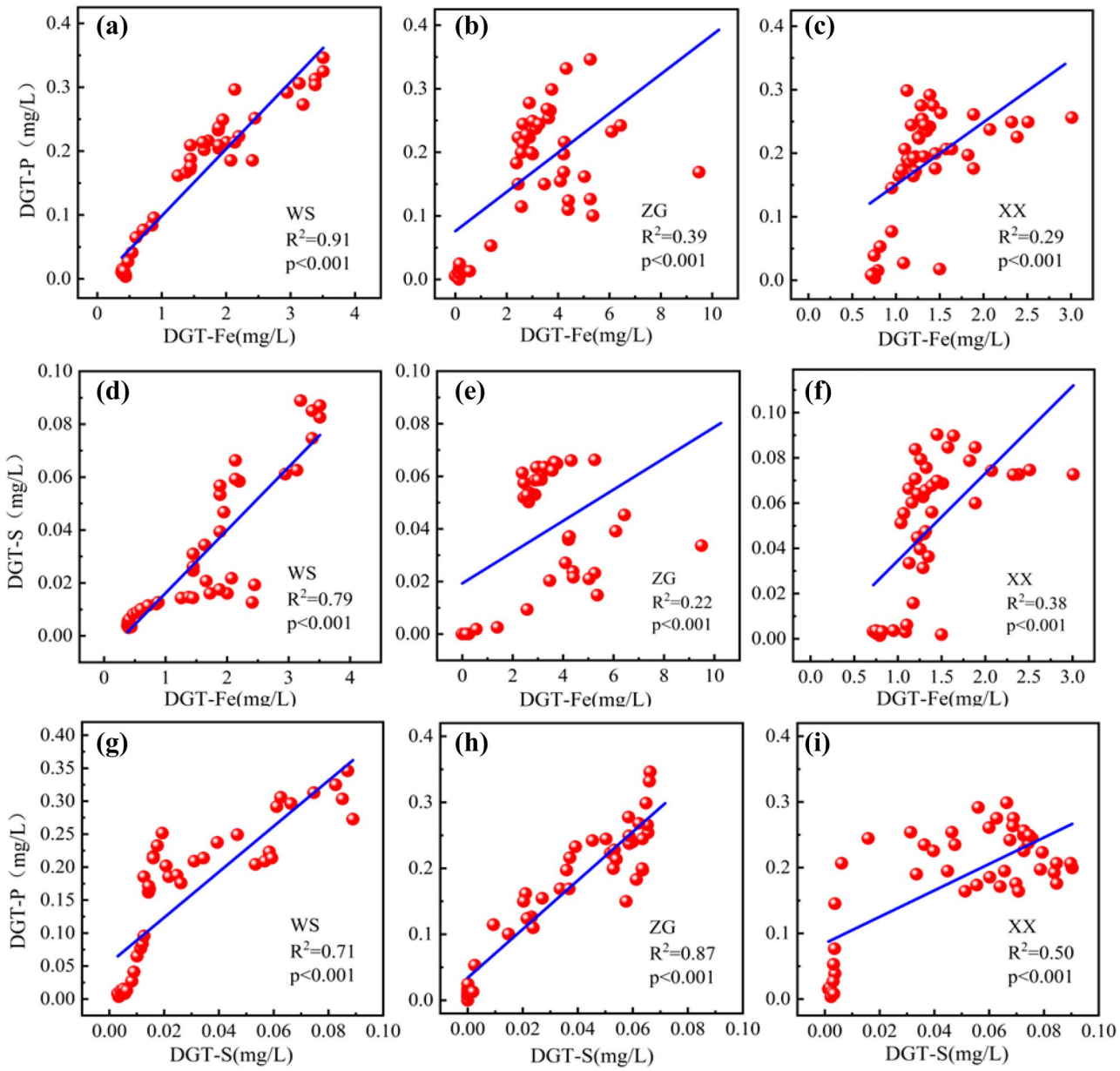

Fig. 6 Concentration correlations between DGT-P and DGT-Fe, DGT-S and DGT-Fe, and DGT-P and DGT-S at the sediment−water interface (SWI) of the sampling sites (WS, ZG, and XX) of the Three Georges Reservoir (TGR) in China

the release of iron-bound P from the sediment (Wang et al. 2016b, 2018b). It was observed that more P is released into the porewater through the reductive dissolution of Fe (III) minerals at the SWI site. In summary, the significant positive correlation between DGT- P, DGT- Fe, and DGT- S in the sediment of the TGR suggests that the reduction of sulfate induces the reductive dissolution of iron-bound P, which is the main mechanism of sediment P release observed in this study.

4 Conclusion

The findings of this study indicate that the sediment in the TGR is characterized by significant internal P load. The decreasing order of P contents of different fractions in sediments is HCl-P > NaOH-P > BD-P. The high-resolution in situ passive sampling monitoring shows that an average P release flux at the SWI is 0.42 mg m^{-2} day^{-1}. The observation, therefore, indicates that sediment release

is an important P source and highlights the importance and urgency of internal P pollution control in the TGR. Furthermore, the reduction and dissolution of Fe–P are the dominant mechanisms responsible for the release of P from the sediments. As the operation cycle of the TGR progresses, P pollutants in the basin will continuously accumulate in the sediment, which will otherwise increase the risk of internal P input. The results of the present study, therefore, scientifically validate the need for the development of internal P pollution control strategies in large deep reservoirs.

Acknowledgements We thank Shuoru Qiu for his help in sample collection and manuscript revision.

Funding Support was provided by the National Key R&D Plan of China (2021YFC3201000), the Strategic Priority Research Program of CAS (No. XDB40020400), the Chinese NSF project (No. 41977296, 42277253), the Guizhou Provincial 2019 Science and Technology Subsidies (No. GZ2019SIG), and the Youth Innovation Promotion Association CAS (No. 2019389).

Declarations

Conflict of interest The authors declare no competing interests.

References

Ahlgren J, Tranvik L, Gogoll A, Waldeback M, Markides K, Rydin E (2005) Sediment depth attenuation of biogenic phosphorus compounds measured by ^{31}P NMR. Environ Sci Technol 39(3):867–872

Andrieux-Loyer F, Philippon X, Bally G, Kérouel R, Youenou A, Le GJ (2008) Phosphorus dynamics and bioavailability in sediments of the Penzé Estuary (NW France): in relation to annual P-fluxes and occurrences of Alexandrium Minutum. Biogeochemistry 88:213–231

Bao Y, Gao P, He X (2015) The water-level fluctuation zone of Three Gorges Reservoir — a unique geomorphological unit. Earth Sci Rev 150:14–24

Chen MS, Ding SM, Chen X, Sun Q, Fan XF, Lin J, Ren MY, Yang LY, Zhang CS (2018) Mechanisms driving phosphorus release during algal blooms based on hourly changes in iron and phosphorus concentrations in sediments. Water Res 133:153–164

Chen Q, Chen JA, Wang JF, Guo JY, Jin ZX, Yu PP, Ma ZZ (2019) In situ, high-resolution evidence of phosphorus release from sediments controlled by the reductive dissolution of iron-bound phosphorus in a deep reservoir, southwestern China. Sci Total Environ 666:39–45

Chen Q, Ni Z, Wang S, Guo Y, Liu S (2020) Climate change and human activities reduced the burial efficiency of nitrogen and phosphorus in sediment from Dianchi Lake. China J Clean Prod 274:122839

Christophoridis C, Fytianos K (2006) Conditions affecting the release of phosphorus from surface lake sediments. J Environ Qual 35:1181–1192

Correll DL (1998) The role of phosphorus in the eutrophication of receiving waters: a review. J Environ Qual 27(2):261–266

De VI, Lopez R, Pozo I, Green AJ (2012) Nutrient and sediment dynamics in a Mediterranean shallow lake in southwest Spain. Limnetica 31(2):231–249

Ding SM, Sun Q, Xu D, Jia F, He X, Zhang CS (2012) High-resolution simultaneous measurements of dissolved reactive phosphorus and dissolved sulfide: the first observation of their simultaneous release in sediments. Environ Sci Technol 46(15):8297–8304

Ding SM, Han C, Wang YP, Yao L, Wang Y, Xu D, Sun Q, Williams PN, Zhang CS (2015) In situ, high-resolution imaging of labile phosphorus in sediments of a large eutrophic lake. Water Res 74:100–109

Ding SM, Wang Y, Wang D, Li YY, Gong MD, Zhang CS (2016) In situ, high-resolution evidence for iron-coupled mobilization of phosphorus in sediments. Sci Rep 6:24341

Gao B, Chen YL, Xu DY, Sun K, Xing BS (2023) Substantial burial of terrestrial microplastics in the Three Gorges Reservoir. China Commun Earth Environ 4:32

Hupfer M, Gachter R, Giovanoli R (1995) Transformation of phosphorus species in settling seston and during early sediment diagenesis. Aquat Sci 57(4):305–324

Jiang X, Jin XC, Yang Y, Li LH, Wu FC (2008) Effects of biological activity, light, temperature and oxygen on phosphorus release processes at the sediment and water interface of Taihu Lake. China Water Res 42(8–9):2251–2259

Lei P, Zhu J, Zhong H, Pan K, Zhang L, Zhang H (2021) Distribution of nitrogen and phosphorus in pore water profiles and estimation of their diffusive fluxes and annual loads in Guanting reservoir. Northern China Bull Environ Contam Toxicol 106(1):10–17

Lewis WM, Wurtsbaugh WA, Paerl HW (2011) Rationale for control of anthropogenic nitrogen and phosphorus to reduce eutrophication of inland waters. Environ Sci Technol 45:10300–10305

Li R, Li Y, Li B, Fu DJ (2021) Landscape change patterns at three stages of the construction and operation of the TGP. Sci Rep 11:9288

Liu C, Wang QX, Watanabe M (2006) Nitrogen transported to three Gorges Dam from agroecosystems during 1980–2000. Biogeochemistry 81(3):291–312

Luo WG, Luo X, Lu J, Bo M (2022) Contribution of the reservoir backflow to the eutrophication of its tributary: a case study of the Xiangxi River. China Hydrol Res 53(3):467–482

Maavara T, Parsons CT, Ridenour C, Stojanovic S, Duerr HH, Powley HR, Van CP (2015) Global phosphorus retention by river damming. Proc Natl Acad Sci USA 112(51):15603–15608

Moore PA, Reddy KR, Fisher MM (1998) Phosphorus flux between sediment and overlying water in Lake Okeechobee, Florida: spatial and temporal variations. J Environ Qual 27(6):1428–1439

Mu Z, Wang Y, Wu J, Cheng Y, Lu J, Chen C, Zhao F, Li Y, Hu M, Bao Y (2020) The influence of cascade reservoir construction on sediment biogenic substance cycle in Lancang River from the perspective of phosphorus fractions. Ecol Eng 158:106051

Mueller S, Mitrovic SM (2015) Phytoplankton co-limitation by nitrogen and phosphorus in a shallow reservoir: progressing from the phosphorus limitation paradigm. Hydrobiologia 744(1):255–269

Mulligan M, Soesbergen A, Saenz L (2020) GOODD, a global dataset of more than 38,000 georeferenced dams. Sci Data 7:1

Murphy J, Riley JP (1962) A modified single solution method for the determination of phosphate in natural waters. Anal Chim Acta 26:31–36

Paytan A, Roberts K, Watson S, Peek S, Chuang PC, Defforey D, Kendall C (2017) Internal loading of phosphate in Lake Erie Central Basin. Sci Total Environ 579:1356–1365

Roden EE, Zachara JM (1996) Microbial reduction of crystalline iron (III) oxides: influence of oxide surface area and potential for cell growth. Environ Sci Technol 30:1618–1628

Rydin E (2000) Potentially mobile phosphorus in Lake Erken sediment. Water Res 34:2037–2042

Schindler DW, Carpenter SR, Chapra SC, Hecky RE, Orihel DM (2016) Reducing phosphorus to curb Lake eutrophication is a success. Environ Sci Technol 50:8923–8929

Sun SJ, Huang SL, Sun XM, Wen W (2009) Phosphorus fractions and its release in the sediments of Haihe River. China J Environ Sci 21(3):291–295

Tu L, Jarosch K, Schneider T, Grosjean M (2019) Phosphorus fractions in sediments and their relevance for historical Lake eutrophication in the Ponte Tresa basin (Lake Lugano, Switzerland) since 1959. Sci Total Environ 685:806–817

Ullman WJ, Aller RC (1982) Diffusion coefficients in nearshore marine sediments. Limnol Oceanogr 27:552–556

Ullman WJ, Sandstrom MW (1987) Dissolved nutrient fluxes from the nearshore sediments of Bowling Green Bay, central Great Barrier Reef Lagoon (Australia). Estuar Coast Shelf Sci 24:289–303

Wang YC, Niu FX, Xiao SB, Liu DF, Chen WZ, Wang L, Yang ZJ, Ji DB, Li GY, Guo HC, Li Y (2015) Phosphorus fractions and its summer's release flux from sediment in the China's Three Gorges Reservoir. J Environ Inform 25(1):36–45

Wang Y, Ding SM, Gong MD, Xu SW, Xu WM, Zhang CS (2016a) Diffusion characteristics of agarose hydrogel used in diffusive gradients in thin films for measurements of cations and anions. Chim Acta 945:47–56

Wang JF, Chen JA, Ding SM, Guo JY, Christopher D, Dai ZH, Yang HQ (2016b) Effects of seasonal hypoxia on the release of phosphorus from sediments in deep-water ecosystem: a case study in Hongfeng reservoir, Southwest China. Environ Pollut 219:858–865

Wang Y, Ding SM, Shi L, Gong MD, Xu SW, Zhang CS (2017) Simultaneous measurements of cations and anions using diffusive gradients in thin films with a Zro-Chelex mixed binding layer. Anal Chim Acta 972:1–11

Wang SL, Li JS, Zhang B, Spyrakos E, Tyler AN, Shen Q, Zhang FF, Kutser T, Lehmann MK, Wu YH, Peng DL (2018a) Trophic state assessment of global inland waters using a MODIS-derived Forel-Ule index. Remote Sens Environ 217:444–460

Wang JF, Chen JA, Guo JY, Sun QQ, Yang HQ (2018b) Combined Fe/P and Fe/S ratios as a practicable index for estimating the release potential of internal-P in freshwater sediment. Environ Sci Pollut Res 25(11):10740–10751

Wang YT, Zhang TQ, Zhao YC, Ciborowski JJH, Zhao YM, O'Halloran IP, Qi ZM, Tan CS (2021) Characterization of sedimentary phosphorus in Lake Erie and on-site quantification of internal phosphorus loading. Water Res 188:116525

Wu J, Huang J, Han X, Xie Z, Gao X (2003) Three-Gorge Dam-Experiment in habitat fragmentation? Sci 300(5623):1239–1240

Wu YH, Wang XX, Zhou J, Bing HJ, Sun HY, Wang JP (2016) The fate of phosphorus in sediments after the full operation of the Three Gorges Reservoir, China. Environ Pollut 214:282–289

Wu T, Qin B, Brookes JD, Yan W, Ji X, Feng J (2019) Spatial distribution of sediment nitrogen and phosphorus in Lake Taihu from a hydrodynamics-induced transport perspective. Sci Total Environ 650:1554–1565

Yu W, Yang HQ, Liao CJA, P, Chen Q, Yang YQ, Liu Y (2022) Organic phosphorus mineralization dominates the release of internal phosphorus in a macrophyte-dominated eutrophication Lake. Front Environ Sci 9:812834

Yuan-Hui L, Gregory S (1974) Diffusion of ions in sea water and in deep-sea sediments. Geochim Cosmochim Acta 38(5):703–714

Zhang R, Wang L, Wu F, Song B (2013) Phosphorus speciation in the sediment profile of Lake Erhai, Southwestern China: fractionation and ^{31}P NMR. J Environ Sci 25(6):1124–1130

Zhang M, Chen G, Luo ZT, Sun X, Xu JL (2020) Spatiotemporal variation, seasonal variation, and potential risks of sedimentary heavy metals in a new artificial lagoon in eastern China, 2014–2019. Mar Pollut Bull 157:111370

Zhou TY, Wan Q, Chai BB, Lei XH, He LX, Chen B (2023) Microbial pathways in the coupling of iron, sulfur, and phosphorus cycles at the sediment–water interface of a river system: An in situ study involving the DGT technique. Sci Total Environ 863:160855

Zhu J, Song C, Wang J, Ke L (2020) China's inland water dynamics: the significance of water body types. Proc Natl Acad Sci USA 117(25):13876–13878